Transfer Properties in Recycled Aggregates Concrete: Experimental and Numerical Approaches

Arthur Fanara[a,b,*], Luc Courard[a], Frédéric Collin[a], Julien Hubert[a]

[a] *Geotechnical Engineering, Urban and Environmental Engineering, University of Liege, Belgium*
[b] *FNRS-F.R.I.A, Fonds de la Recherche Scientifique, Belgium*

Abstract

This paper analyses the influence of Recycled Concrete Aggregates (RCA) on durability through a study of transfer properties of concrete, using a coupled approach consisting of experimental testing and numerical modelling.

Experimental tests performed on concrete made from Natural Aggregates (NA) or RCA conclude that Recycled Aggregate Concrete (RAC) is more porous than its NA-based counterpart. Its water absorption is also superior while its intrinsic permeability is slightly lower than regular concrete.

A coupled thermo-hydraulic numerical model, based on non-linear finite elements and constitutive equations, is developed. These constitutive equations rely on properties determined experimentally, on concretes made in the laboratory. The results disclose that RAC has a saturation degree constantly above the one of regular concrete.

Keywords: Durability, Finite Element Analysis, Transport Properties, Recycled Aggregates, Modelling, Waste Management

1. Introduction

Concrete structures are built to withstand the effects of time: most of them are built to reach a service life of more than a 100 years. Over its service life, concrete undergoes many degradation processes: freeze-thaw cycles, carbonation, chloride attack and alkali-aggregate

*Corresponding author.
Email addresses: arthur.fanara@uliege.be (Arthur Fanara), luc.courard@uliege.be (Luc Courard), f.collin@uliege.be (Frédéric Collin), julien.hubert@uliege.be (Julien Hubert)

reaction among others. Those degradation processes, applied to the concrete either directly or indirectly, are often coupled and can interact, reducing service life [1, 2].
In most of the cases (e.g. chloride attack), water is required to initiate or support degradation processes [3]. This is why this research focuses on the transfer properties that promote the penetration of the several ions species known to cause degradation processes.

Due to the long period of time involved, studying the durability of concrete requires numerical modelling. Furthermore, modelling can help understand the transfers of water and vapour inside concrete, which are complex processes influenced by various parameters, such as moisture distribution.
Moisture distribution influences various processes in concrete [4]. To represent the amount of moisture, one can use relative humidity (RH) instead of the moisture content itself, simplifying the numerical analysis [5, 6, 7].

One of the most cited moisture models for concrete, in the literature, is Bažant and Najjar's (1972) physical model, based on a nonlinear diffusion equation [5]. In their model, they state that "*the equations governing drying and wetting of concrete are formulated assuming the diffusivity and other material parameters to be dependent on pore humidity, temperature and degree of hydration*" [5]. Drying of concrete is then described by the following second-order equation, if a one-dimensional problem along the coordinate x is assumed and without variation of temperature [8]:

$$\frac{\partial w}{\partial h}\frac{\partial h}{\partial t} - \frac{\partial}{\partial x}\left(D_h \frac{\partial h}{\partial x}\right) - \frac{\partial h_s}{\partial t} = 0 \tag{1}$$

where w [-] is the moisture content, h [-] is the pore relative humidity and h_s [-] a function describing self-desiccation. The ratio $\partial w/\partial h$ represents the slope of a sorption isotherm, while the coefficient D_h [m^2/s] is the moisture diffusivity.

Parrott (1988) developed another empirical model for concrete drying, where moisture content is described as a function of the water-to-cement ratio and the ambient relative

humidity [9].

In 1994, Xi et al. adapted the Bažant and Najjar model by introducing the BET model for sorption isotherms developed by Brunauer et al. in 1938 [10, 11], therefore resolving the issue of the linear function for sorption isotherms. They also defined the moisture diffusivity as a function of the W/C ratio, and the sorption isotherms were linked to the W/C ratio, type of cement, temperature and age of concrete.

Xi et al. (1994) also derived an expression of the moisture diffusivity based on experimental data fitting [12]:

$$D_h = \alpha_h + \beta_h \left[1 - \exp\left(-10^{\gamma_h^{(h-1)}} \ln(2)\right)\right] \tag{2}$$

where the three parameters α_h, β_h and γ_h are functions of the water-to-cement ratio.

One of the last models is the Baroghel-Bouny's one (2007) which is based on an extensive experimental work during which the influence of the water-to-cement ratio on the moisture properties, microstructural characteristics and transport properties was studied [13].

In this research, the model used is quite similar to the one expressed in the Equation 1 as it also solves the mass balance equation. However, properties used are not dependent on the W/C ratio, type of cement, and so on but they are rather obtained from experimental results on the concrete. Indeed, the mass balance equation of water used is the following [14, 15]:

$$\frac{\partial\left(\rho_w \, n \, S_{r,w}\right)}{\partial t} + div\left(\rho_w \, \underline{f_w}\right) - Q = 0 \tag{3}$$

where ρ_w [kg/m^3] is the water density, n [-] the porosity, $S_{r,w}$ [-] the water saturation degree, t [s] the time, Q [kg/s] is the injected flux and $\underline{f_w}$ is the Darcy's flow. Another intrinsic property used in this equation is the intrinsic permeability, through the Darcy's flow.

Among the many parameters cited, the composition of concrete is obviously playing a significant role in the transfer processes. Aggregates account for around 75% of the overall

concrete volume. Their properties therefore have a strong influence on its performance and it is required that these aggregates comply with several chemical, geometrical and physical properties [16]. Recently, the environmental impacts and extensive use of natural resources by the construction industry have raised concerns. A new type of material has therefore been studied in response: the Recycled Concrete Aggregates (RCA). Those RCA, obtained by crushing of old concrete structures, are composed of Natural Aggregates (NA) and a part of adherent mortar paste, the latter impairing their properties compared to those of NA [17, 18].

The standards currently used in the construction industry are based on natural aggregates, and it is therefore harder for the recycled concrete aggregates to abide by those. Further numerical modelling could therefore help develop standards relative to RCA, allowing their implementation in more and more applications.

Concrete made with recycled concrete aggregates has often been investigated from a mechanical point of view [19, 20, 21, 22] rather than for its durability aspects [23, 24, 25, 26]. Recent work has nonetheless been done on RCA, trying to model various properties of concrete. Among others, Lovato et al. (2012) and Biglarijoo et al. (2017) used the response surface methodology (RSM) to model the results of various experimental tests: water absorption, carbonation depth, tensile and compressive strength, density among other properties of concrete [20, 21].

Approaching the Recycled Aggregate Concrete from a transfer point-of-view, this work answers the scientific question: "Is it possible to efficiently model water transfer in Recycled Aggregate Concrete ?"

To reach that goal, a better understanding of the material behaviour is required: an extensive experimental programme is conducted. Modelling of the various transport phenomena inside concrete is then performed to promote the use of RCA in concrete, allowing the prediction of a possible loss of durability of concrete produced with recycled concrete aggregates. As shown in the literature, there is indeed little research done in the field of modelling the

transfer phenomena happening in recycled aggregates concrete.
The modelling is performed with a nonlinear finite elements software developed at the University of Liège (called Lagamine) [27, 28]. It follows the theory of nonlinear finite elements modelling of flows in porous media and consists of a coupled thermo-hydraulic study of the material [27].

The novelty of this research stems from the combined experimental and numerical approach. Concretes made from NA or 100% RCA in the laboratory, with the only purpose of studying the substitution of aggregates, are thoroughly characterized through an experimental programme. It allows a clearer understanding of the transfer processes as a lot more parameters are controlled compared to compositions that would come from existing sites for example. The obtained results are fed to a validated numerical model, predicting the influence of the substitution of aggregates on the durability of concrete. Due to the composition method, the conclusions drawn are solely due to the substitution of aggregates, allowing a clearer understanding of the effects at play.

2. Materials and Methods

2.1. Recycled Concrete Aggregates (RCA)

The first parameter that impacts the quality of the recycled concrete aggregates is their method of production. RCA are produced by crushing of old concrete elements after demolition of outdated structures. Various fragmentation techniques are available to turn those elements into aggregates: impact crusher, jaw crusher or cone crusher among the most used ones. They all have their advantages and drawbacks, more specifically in terms of aggregates' size and morphology, production of fines and energy consumption [29].
Moreover, the crushing process produces microcracks, thereby rendering the recycled aggregate concrete more prone to capillary absorption [30]. RCA are indeed composed of NA (65-70% by volume) embedded in a hardened, porous and cracked cement matrix (30-35% by volume), yielding a higher water absorption than natural aggregates. Research has proven

that RCA have a lower density, higher porosity and water absorption capacity and lower Los Angeles abrasion coefficient than NA. They are, furthermore, more complex and heterogeneous by nature [31, 25, 32, 33, 18, 34, 35].

Several internal parameters influence the amount of residual mortar in RCA, among which are the initial paste content and its properties, as well as the mechanical quality of the transition zone (ITZ) at the interface between the initial natural aggregates and the cement paste. The crushing process and considered particle size of the RCA are also influencing the amount of adherent cement paste, but are considered external parameters [33, 36, 16].

According to the literature, the amount of adherent mortar found in coarse RCA decreases when the diameter of the RCA increases. It was found that 4/8mm fractions have a mortar content ranging from 33% to 55% (by weight) while bigger 8/16mm fractions have a mortar content in between 23% to 44% [17, 33, 37].

The negative effects of RCA are therefore more marked for fine aggregates than for coarse aggregates [38], mainly because recycled fine aggregates are composed of more cement paste than coarser ones [16].

Because the worst properties of the RCA come from their adherent mortar content, the greater it is and the greater the water absorption is [17]. Furthermore, the greater the substitution ratio of NA by RCA in the concrete, the bigger its water absorption and porosity [39], which in parallel decreases the durability of the concrete [38].

Chemical compatibility between the new cement paste and the residual one of the RCA may be an issue and impact the properties of concrete [36]. Recycled concrete is often contaminated by several sources of aggressive ions (sulphates, chlorides, ...) coming from deicing salts or sewage/sea water among others. These pollutants may thus alter the properties of the concrete made from RCA in both its fresh and hardened state, decreasing its durability [25].

One of the main properties of RCA which is of major interest with respect to this research is the water absorption. Water absorption is correlated with morphological and mechanical properties of aggregates [40]. It has been found that the water absorption ranges from 3 to 12% for RCA, which is significantly greater than the values for NA, ranging from 0.5 to 2% [31, 36, 18].

2.2. Concrete Compositions: C-NA and C-RCA

Two concrete compositions were used to characterize the influence of substituting natural aggregates (NA) by recycled concrete aggregates (RCA) in concrete. The reference concrete was obtained through the application of the Dreux-Gorisse method [41] and named C-NA. Then, the NA were substituted by RCA with a constant volume method to obtain the C-RCA, whose only difference is the substitution of aggregates. That means that the volume is constant but the mass is proportional to the bulk density of the aggregates.

The cement type used in both compositions is a CEM I 42.5 N and the sand is a 0/4 screed sand. The natural aggregates are crushed limestone aggregates 2/7 while the recycled concrete aggregates are of sizes 0/4, 4/6.3 and 6.3/8 mixed to obtain the same granulometric curve as the NA. The percentage of each fraction is given in Table 1.
The Recycled Concrete Aggregates are sourced from our laboratory at the University of Liège. Parent concrete was made in the laboratory, then crushed with a jaw crusher and stored inside. It allows us to alleviate a larger number of unknowns by controlling the origin, storage conditions and conditioning of the RCA. Furthermore, both the NA and RCA have not been pre-soaked prior to the mixing, and both were stored in a room with the same relative humidity and temperature.

Diameter (mm)	Percentage of mass (%)
2/4.0	48
4/5.0	22.9
5/6.3	20
6.3/8	9.1

Table 1: Fractions used to mimic the granulometric curve of the natural aggregates

The mass of recycled concrete aggregates required (in [kg/m^3]) was calculated by the following formula:

$$M_{\text{RCA}} = V_{\text{aggregates,C-NA}}\ \rho_{\text{RCA}} = P_{\text{C-NA}}\ \frac{\rho_{\text{RCA}}}{\rho_{\text{NA}}} \tag{4}$$

where $P_{\text{C-NA}}$ ([kg/m^3]) is the required mass of aggregates found by the Dreux-Gorisse method for the reference concrete. The bulk density of the recycled aggregates and natural aggregates used are respectively 2290kg/m^3 and 2590kg/m^3.

In addition to the mass of aggregates which is modified to consider the change from NA to RCA, the amount of water required is also updated to account for the absorption and water content of the RCA. Those parameters were measured according to EN 1097-5 and EN 1097-6 standards. An absorption of 7.92% and a water content of 5.45% were obtained for the RCA, compared to 1.24% and 0.16%, respectively, for the NA.
This difference in the water content will change the water-to-cement ratio. However the quantity of efficient water, that is water to be consumed by the reaction of hydration and not by absorption by the aggregates, is constant. The efficient water-to-cement ratio is therefore equal for both compositions.

The two final compositions used are shown in Tables 2 and 3, where the total and efficient water-to-cement ratios can be observed, as well as the results from the slump test performed. Both compositions have an identical efficient W/C ratio and slump, comforting our method of composition to obtain two concretes with the same matrix but different aggregates.

C-NA	
Water	226.2 kg/m^3
Cement	432.5 kg/m^3
Sand	575.9 kg/m^3
Aggregates	1065.4 kg/m^3
Total W/C ratio	0.523
Efficient W/C ratio	0.496
Slump test	180mm (S4)

Table 2: C-NA Composition

C-RCA	
Water	237.9 kg/m^3
Cement	432.5 kg/m^3
Sand	575.9 kg/m^3
Aggregates	941.9 kg/m^3
Total W/C ratio	0.550
Efficient W/C ratio	0.496
Slump test	175mm (S4)

Table 3: C-RCA Composition

2.3. Water Absorption by Immersion

The Water Absorption by Immersion (WAI) test gives an indication of the water absorption and porosity of the sample. The modus operandi is dictated by the Belgian standard NBN B 15-215:2008 (water absorption specifically for concrete) and NBN EN 772-4 (densities and porosity for masonry).

The samples (forty $100 \times 100 \times 10$mm square plates) are weighed three times:

- Once completely saturated:

194 – Under water to obtain the submerged saturated mass ($m_{sat,w}$);

195 – In the air, after being wiped with a damped cloth, to obtain the saturated mass
196 ($m_{sat,a}$);

197 • Once completely dried in a heat chamber at 105 °C (m_{dry}).

198 The water absorption, noted WA [% mass], is obtained by the following relation between
199 the humid and dry mass:

$$\mathrm{WA} = \frac{m_{sat,a} - m_{dry}}{m_{dry}} \times 100 \tag{5}$$

200 Another indicator of durability available through the WAI test is the porosity accessible
201 to water, noted n_w [% volume]:

$$n_w = \frac{m_{sat,a} - m_{dry}}{m_{sat,a} - m_{sat,w}} \times 100 \tag{6}$$

202 Finally, the dry and humid bulk densities, noted respectively ρ_d and ρ_h, are obtained
203 from the following equations:

$$\rho_d = \frac{m_{dry}}{V_{sample}} = m_{dry} \times \frac{\rho_w}{m_{sat,a} - m_{sat,w}} \tag{7}$$

204

$$\rho_h = \frac{m_{sat,a}}{V_{sample}} = m_{sat,a} \times \frac{\rho_w}{m_{sat,a} - m_{sat,w}} \tag{8}$$

205 *2.4. Static Sorption and Desorption*

206 Sorption and desorption isotherms, as well as water retention curves, may be obtained
207 from static sorption and desorption experiments applying the vapour control technique. It
208 consists of hermetically sealed chambers containing saline solutions to control the relative
209 humidity. The samples hence lose or gain mass to reach a water content at equilibrium with
210 the RH imposed by the saline solution [6, 42].
211 Each chamber contains four 100×100mm square plates of approximately 10mm of thickness
212 for each composition. Before the experiment, the samples used for the sorption are com-
213 pletely dried until constant mass. The desorption requires saturated samples, and those are
214 therefore taken directly from the humid chamber where they were curing. Each plate is

carefully weighed before being put in the chamber.

Approximately once a week (each opening of the chamber disturbs the RH equilibrium), all the samples are weighed and the relative humidity and temperature of their chamber are taken from hygrometric sensors. Those chambers being kept in a room with controlled environment (60% RH and temperature of 21°C), the temperature is not supposed to vary meaningfully. The weighing stops once the mass of the samples is considered constant, with respect to the stabilisation of the RH in the chamber.

At the beginning, and in order to better control and interpret the results, five chambers (each containing a different saline solution) were used for the sorption and desorption. However, due to the longer time required for the chambers 3'-4'-5' to reach a stabilised RH in static desorption, those chambers were split in two, decreasing the number of specimens by two and increasing the speed at which the atmosphere stabilised around a specific relative humidity; the more samples there are in the chamber, the more moisture transfers take place and the slower the equilibrium is reached. Table 4 summarises the saline solutions chosen for each chamber. The choice was oriented to cover the whole range of possible relative humidity.

Saline Solution	**Chamber Id.**	
	Sorption	**Desorption**
KCl	1	1'
NaCl	2	2'
$Ca(NO_3)_2$	3	3' and 3'bis
$MgCl_2$	4	4' and 4'bis
Silica Salt	5	5' and 5'bis

Table 4: Saline solutions used for the static sorption and desorption experiments.

The Kelvin law allows, based on the temperature T [K] and target relative humidity RH

[-], to determine a target suction s [MPa]:

$$s = -\frac{\rho_w \, R \, T}{M} \, \ln(RH) \tag{9}$$

where R is the constant of perfect gases ($R = 8.3143$ J/K.mol), M is the molar mass of water ($M = 18.016$ g/mol) and ρ_w is the density of water.

Once the relative humidity of each chamber is stabilised and the mass of each plate is constant, the experiment stops. The mean water content is then calculated for each composition and for each RH in order to obtain the water retention curves of each composition. The water content requires the dry mass of each plate, and those therefore need to be dried in a heat chamber at 105°C after the experiment (except for the one used in sorption as they started dry).

2.5. Water permeability

Water permeability is an important property of concrete: it is defined as the ability of fluids to penetrate and migrate inside the porous medium.

The measurement of water permeability is done in a triaxial cell, accordingly to the standard NBN EN ISO 17892-11:2019. The samples used are cylinders of approximately 100mm diameter and 100mm height, initially saturated as they are stored in a humid chamber and then in a water bucket before testing. The sample is then wrapped, along its height, inside a waterproof membrane to force a one directional flow. Both its upper and lower sides are in contact with porous discs to allow water transfer. This sample is then put inside the triaxial cell and a water discharge is forced from the top to the bottom of the sample and controlled to obtain a constant pressure difference of 200kPa: this method is called the constant-head method. As concrete is poorly deformable, the macro-porosity on the lateral sides of the sample is filled with plaster in order to decrease the risk of microperforation of the waterproof membrane.

Once the in-flow discharge is equal to the out-flow one, the saturated conductivity can be determined based on the Darcy's law under the hypothesis of a permanent flow in saturated porous media [43]:

$$K_{sat} = \frac{Q}{i \times A} = \frac{Q}{A} \times \frac{H}{\Delta h} \tag{10}$$

with K_{sat} the water-saturated conductivity [m/s], Q the discharge [m^3/s], i the hydraulic gradient [-] and A the cross-sectional area of the member [m^2]. The hydraulic gradient is calculated as the ratio of the hydraulic head (Δh [m]) over the height of the sample (H [m]). The discharge is not measured directly, but a volume of water going through the sample is measured at certain times and then the discharge can be determined from the ratio of the volume over the elapsed time.

This value of water-saturated conductivity is highly dependent on the temperature and will therefore be transformed into a generic value at 10°C. Finally, once this conductivity has been calculated, the intrinsic permeability [m^2] can be obtained:

$$k_{int} = K(10°\text{C}) \times \frac{\mu_w}{\rho_w \, g} \tag{11}$$

where μ_w is the viscosity of water (equal to 1.0016 [MPa/s] at 20°C) and g is the gravitational force (equal to 9.81 [m/s^2]).

3. Results and Interpretation

3.1. Water Absorption by Immersion

The Water Absorption by Immersion (WAI) test yielded results in terms of densities, water absorption and porosity. The densities of each composition are shown in Table 5 with their standard deviations. One can see both the dry and humid densities obtained from the WAI experiment. As expected, the RCA displaying a lower density than the NA, the density of the resulting concrete is also lower for the C-RCA than for the C-NA.

Table 5 also shows the results in terms of water absorption and porosity. As it was mentioned before, concrete made from RCA has a greater porosity and therefore greater water

absorption. However, the measure of the porosity is not as accurate as one could expect as it only represents the porosity accessible to water.

Composition	**Dry density** [kg/m^3]	**Humid density** [kg/m^3]	**Water Absorption** [% mass]	**Porosity** [% volume]
C-NA	2220±11	2376±9	7±0.2	15.6±0.3
C-RCA	2033±9	2238±7	10.1±0.2	20.5±0.3

Table 5: Results yielded by the WAI test: density, water absorption and porosity.

It is known that the recycled concrete aggregates have a higher water absorption than the natural aggregates. The water absorption of both aggregates has been measured before mixing the compositions and it is therefore possible to correlate the difference in water absorption between the C-NA and C-RCA (written WA_c) with the difference in water absorption of their respective aggregates (corrected respectively for the mass used in the composition and noted WA_a):

$$\begin{cases} \Delta\mathrm{WA}_c = \mathrm{WA}_{\text{C-RCA}} - \mathrm{WA}_{\text{C-NA}} = 10.1 - 7 = 3.1\% \\ \Delta\mathrm{WA}_a = \mathrm{WA}_{\text{RCA}} - \mathrm{WA}_{\text{NA}} = 3.41 - 0.57 = 2.84\% \end{cases} \tag{12}$$

which are close enough to validate that the two compositions will mainly exhibit differences due to the differences in aggregates properties, and not because of mortar matrix differences.

3.2. Static Sorption

The evolution of the relative humidity inside each chamber with respect to time can be seen in Figure 1. One can observe in dash-dot line the RH targeted inside each chamber and then, in simple line, the actual value of the RH inside each chamber. Moreover, for the static desorption, the chambers 3'-4'-5' have been doubled in order to speed up the process: the dash line represents each new chamber (starting from day 10).

The values of the RH at equilibrium are not always equal to the values predicted, especially for low RH. Moreover, the chambers used for the static sorption have been stabilised long before the ones for the static desorption as the conditions are easier to work with (saturation

304 of the sample instead of desaturation). The values of the RH and suction obtained are shown
305 in Table 6.
306

Chamber id.	**Saline solution**	**Equilibrium**	
		RH [%]	**Suction** [MPa]
Static Sorption			
1	KCl	83.11	25.27
2	NaCl	75.7	38.07
3	$Ca(NO_3)_2$	57.04	76.76
4	$MgCl_2$	40.22	124.56
5	Silica salt	11.5	295.24
Static Desorption			
1'	KCl	84.4	25.25
2'	NaCl	76.88	38.09
3' and 3'bis	$Ca(NO_3)_2$	76.4 and 65.93	36.82 and 56.91
4' and 4'bis	$MgCl_2$	36.86 and 60.38	136.42 and 69.02
5' and 5'bis	Silica salt	44.96 and 22.57	109.03 and 203.17

Table 6: Saline solutions used for the static sorption and desorption experiments: equilibrium RH and suction.

307 As one can also see, the measurements were initially done once a week but were then
308 spaced out to minimise disruption of the chambers and give more time to the samples to
309 reach a constant mass.
310

311 Based on the value of the RH and the final mass of each sample, it is possible to determine
312 the saturation degree corresponding to each suction in order to draw the Water Retention
313 Curve (WRC) for each composition. The WRC represents the evolution of the degree of
314 saturation with respect to the suction. They are then used to fit the Van Genuchten model

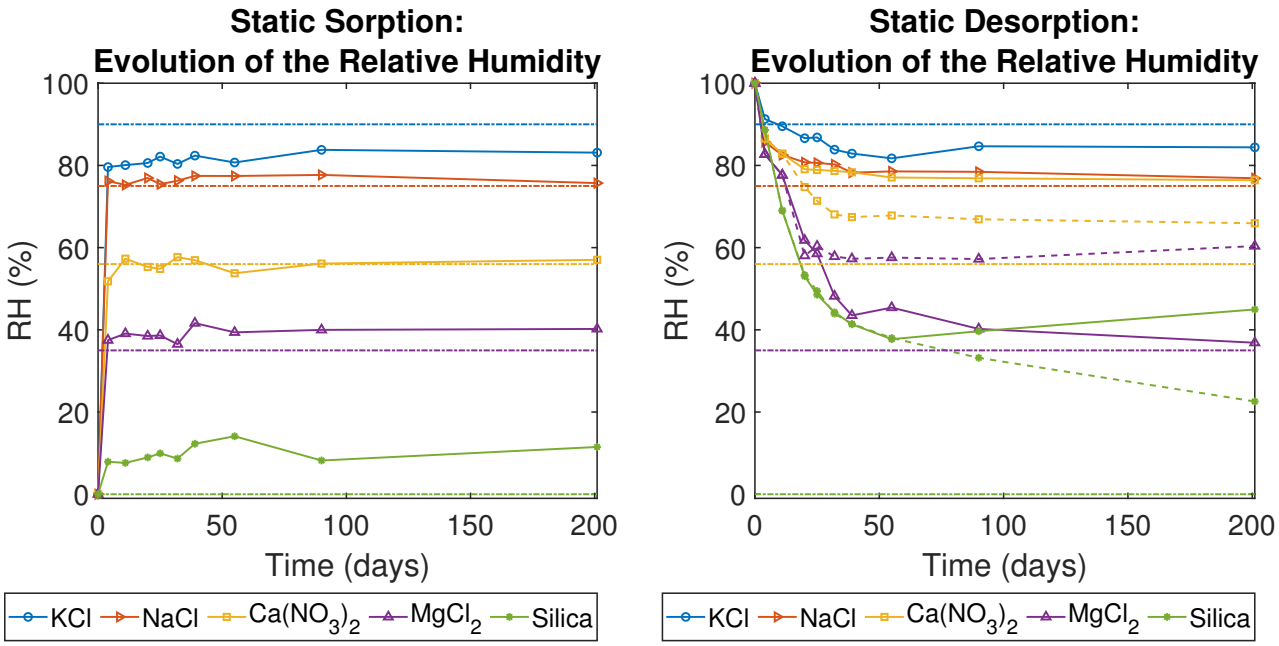

Figure 1: Evolution of the Relative Humidity inside each chamber towards a target RH.

to be used in the modelling aspect of this paper [7]:

$$S_{r,w} = S_{res} + (S_{sat} - S_{res}) \left(1 + \left(\frac{s}{\alpha_{vG}}\right)^{n_{vG}}\right)^{-m_{vG}} \tag{13}$$

$$m_{vG} = 1 - \frac{1}{n_{vG}} \tag{14}$$

where S_{sat} and S_{res} are the maximum and the residual saturations, and s [MPa] is the total suction defined by the Kelvin law in Equation 9. The model parameters are n_{vG} [-], linked to the rate of desaturation of the soil, m_{vG} [-], associated to the curvature (slope) of the water retention curve and α_{vG} [Pa], related to the air-entry pressure [44].

Then, the Van Genuchten model can be fitted on the obtained experimental results (Equation 13) and the relative permeability can also be deduced from this model through the following equation [44]:

$$k_{rel,w} = \sqrt{S_{r,w}} \left(1 - \left(1 - S_{r,w}^{1/m_{vG}}\right)^{m_{vG}}\right)^2 \tag{15}$$

The water retention curves corresponding to the two compositions studied are shown in Figure 2 for the desorption as well as the sorption.

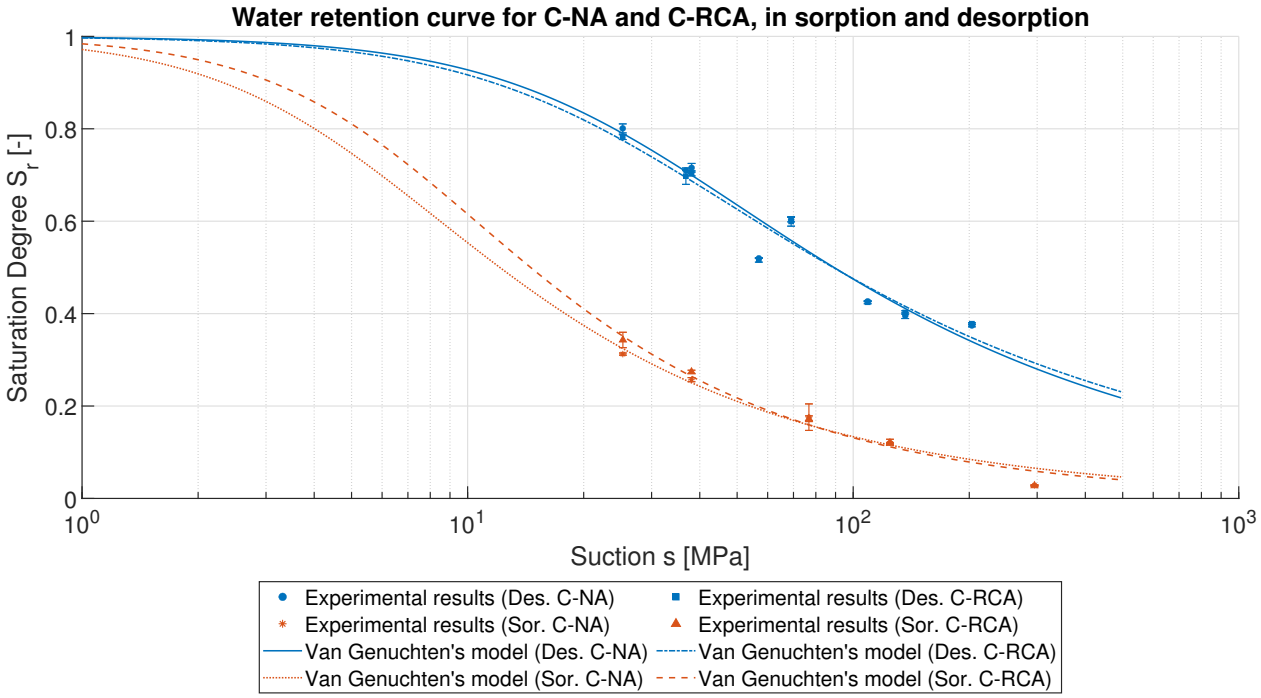

Figure 2: Water retention curve fitted with the Van Genuchten model for C-NA and C-RCA, both in desorption and sorption.

Table 7 summarises the value of all the parameters obtained for each composition, for both the sorption and desorption experiments.

Parameter	C-NA	C-RCA
Static Desorption		
α_{vG} [MPa]	25.08	22.05
n_{vG} [-]	1.51	1.47
m_{vG} [-]	0.34	0.32
Static Sorption		
α_{vG} [MPa]	4.76	6.47
n_{vG} [-]	1.66	1.74
m_{vG} [-]	0.4	0.43

Table 7: Values of the Van Genuchten model's parameters to be used in the modelling and obtained through the static sorption and desorption experiments.

The results show that the use of RCA in concrete reduces the air-entry pressure α_{vG} (for desorption) while having no significant effect on the parameter n_{vG}. It means that, for most values of the suction and more particularly for low suction, the saturation degree will be lower in the C-RCA than in the C-NA. However, one should not forget that the faster a sample desaturates and the lower the relative permeability gets. Therefore, a low-permeability zone is created and the water inside the sample has more difficulty to reach the external surface.

For static sorption results, the curves should be analysed the other way around. Indeed, sorption happens when the relative humidity increases, which in turn decreases the suction. By looking at the curves, one can see that the C-RCA has an increase of its saturation greater than the C-NA, for a same increase of the suction, which is similar to the results of the desorption.
A final remark is that there is clearly a hysteresis in the water retention curve for both compositions.

3.3. Water Permeability

The final experiment whose results are analysed is the water permeability experiment. Two samples were tested for each composition, and the results obtained can be found in Table 8, where one can see the intrinsic permeability for each sample and then the mean value, for each composition studied.

Composition	Intrinsic Permeability [m^2]		
	Sample 1	Sample 2	Mean value
C-NA	2.76E-20	1.26E-19	7.68E-20
C-RCA	8.28E-20	1.27E-20	4.78E-20

Table 8: Water permeability results for both compositions

One can see that the C-RCA is a bit less permeable than the C-NA (nearly 60%), which is a remarkable difference without being excessive.
This slight difference may have two causes. First, the greater absorption of the RCA is said to increase the quality of the ITZ around them due to a smaller bleeding effect, decreasing the permeability locally. Then, the greater porosity of the aggregates may allow a better formation of crystals during the hydration of cement, increasing the quality of the ITZ by reducing the permeability locally [45, 46, 34].

4. Numerical Comparison of C-NA and C-RCA

The numerous parameters determined experimentally are now to be used in the modelling of an arbitrary column; we model a rectangular column of 40cm width for 20cm thick which would be submitted to the environmental conditions on two parallel sides only.
The mesh used for the modelling is displayed at Figure 3. As the transfers occurs symmetrically, only the upper half of the section is represented. The modelling is conducted in a plane strain state.

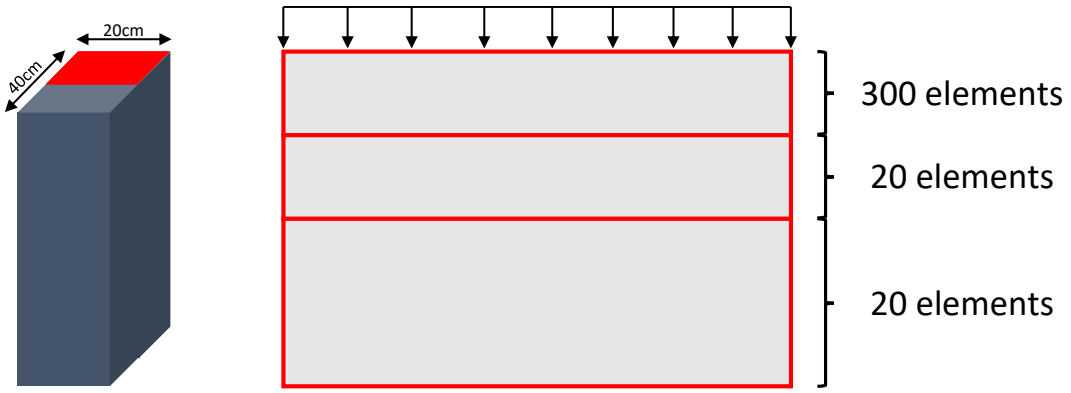

Figure 3: Mesh used for the modelling of the application's column

The relative humidity is based on existing measurements in Brussel, Belgium [47]. A semi-sinusoidal pattern with a period of one year is observed, with the RH varying from 40% to 95% approximately.
Then, according to the data relative to the temperature, it varies from -5°C to 25°C in the same period as the relative humidity, the warmer the environment and the lower the relative humidity. The loading applied to the column section is summarised in Table 9.

The modelling is achieved for a period of five years in order to reach a transitional (due to the varying external conditions) yet kind of permanent regime. Indeed, as the solicitations are changing in the same exact manner every year, the saturation inside the column should change accordingly between single upper and lower values, identical along the years.

Time	**Temp.** [K]	**RH** [%]	**Suction** [MPa]
0-12-24-36-48-60 months	298.15	40%	126.07
6-18-30-42-54 months	268.15	95%	6.35

Table 9: External loading (temperature and suction) applied to the column

Table 10 displays the value of the parameters used for the modelling of the application for both compositions studied. The value of the mass and heat transfer coefficients used were

obtained on C-NA samples during previous convective drying tests. Those transfer parameters are rather important but are not intrinsic parameters of the material used. They mainly depend on the drying conditions (temperature, wind speed, ...) and the sample shape [14]. Therefore, using the same coefficient for the two concretes studied is important, but the exact value of theses parameters is less important.

An important remark is that the environmental conditions applied introduce desorption as well as sorption inside the concrete elements. However, it is not possible to introduce two sets of parameters inside the modelling software. It was thus decided to use the parameters related to the desorption all along the modelling, not taking into account the hysteresis between the sorption and desorption curves.

Parameter	**C-NA**	**C-RCA**	**Experimental source**
Density of the solid grains (ρ_s) [kg/m^3]	2630	2557	Water Absorption by Immersion
Concrete's intrinsic permeability (k_{int}) [m^2]	7.68E-20	4.78E-20	Water Permeability
Concrete porosity (n) [-]	0.156	0.205	Water Absorption by Immersion
Van Genuchten model parameter (m_{vG}) [-]	0.34	0.32	Static Desorption
Van Genuchten model parameter (n_{vG}) [-]	1.51	1.47	Static Desorption
Air entry pressure (α_{vG}) [MPa]	25.08	22.05	Static Desorption
Minimal concrete's relative permeability [-]	1E-4	1E-4	-
Mass transfer coefficient (α) [m/s]	1.99E-3	1.99E-3	Convective Drying
Heat transfer coefficient (β) [W/m^2.K]	2.579	2.579	Convective Drying

Table 10: Parameters used in the modelling of the column under variable relative humidity and temperature for both compositions C-NA and C-RCA.

As a reminder, Figure 4 shows the water retention curve and relative permeability curve for the C-NA and C-RCA. The values of the suctions relative to the external conditions applied are also represented on that figure. One can see a small difference between both compositions: it seems negligible but still induces differences in saturation in the results

obtained.

Figure 5 represents the evolution of the water content with respect to time. The first observation that can be made is that the C-RCA loses more mass than the C-NA due to its higher porosity (and therefore higher initial water content). However, at the beginning of the simulation, the C-RCA loses less water content than the C-NA due to its lower relative permeability.

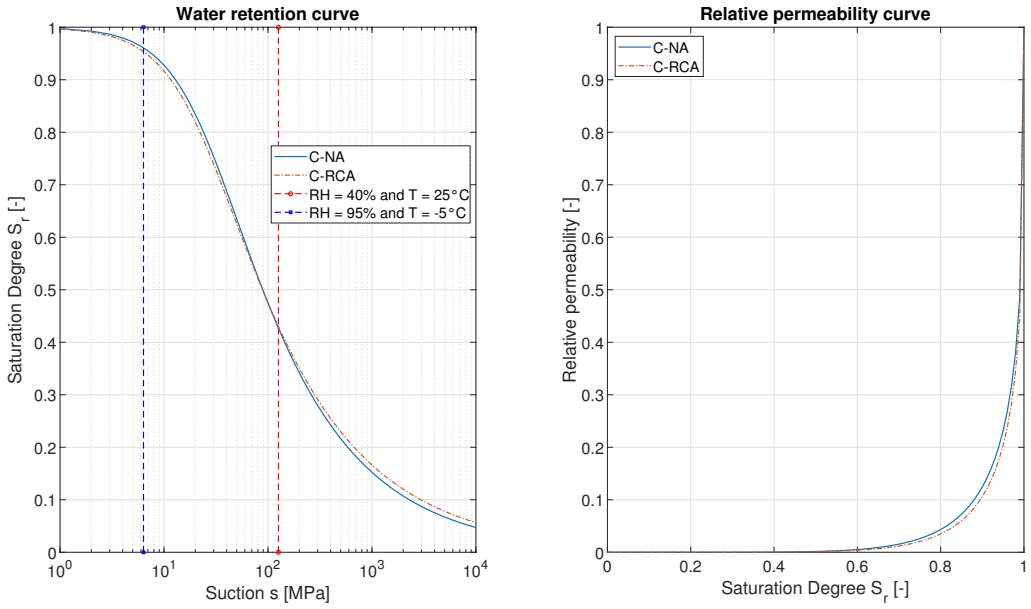

Figure 4: Water retention curve and relative permeability curve for C-NA and C-RCA.

Figure 6 also represents the evolution of the saturation degree along the width of the sample for a period of four months and starting at 36 months of simulation. The purpose of this graph is to better observe the delayed effects of the applied conditions changes. One can see that the saturation increases at the surface while it still decreases near the middle of the sample (or bottom of the mesh in the figure shown). This is mainly due to the water and vapour flows which still go from the more saturated zone to the less saturated one in order to reach an equilibrium in the sample. Even if the surface's saturation increases quickly and therefore the flows nearer to the surface of the sample go from the surface to the inside, the

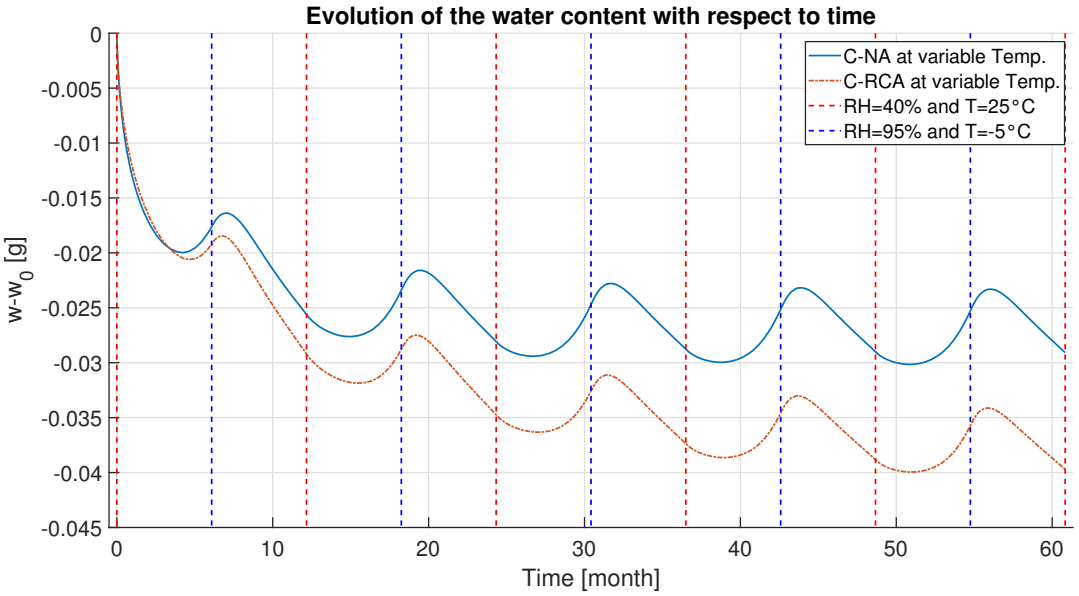

Figure 5: Evolution of the mass with time, for both C-NA and C-RCA.

middle section of the mesh is still less saturated than the inside and therefore the flows near the center go from the inside of the sample to the exposed surface.
In addition to this, one can observe that the C-RCA has a higher saturation degree than the C-NA along the whole section, except at its surface near the end of the sorption phase. It is due to the lower permeability of the C-RCA that decreases water exchanges between the column and its environment.

The same conclusions can be easily made from Figure 7 which shows the evolution, with respect to time, of the saturation degree at various positions inside the column's section. The first position studied is at the exposed surface of the section: the amplitudes of variation are indeed higher than at all the other positions as the exposed surface is in direct contact with the environmental conditions applied. Moreover, the sorption/desorption changes happen directly as the applied conditions change. In terms of compositions, the C-RCA is more saturated than the C-NA all along the simulation, even though the difference is negligible. The next position is at a 100mm from the exposed surface: the amplitudes of the variations are obviously smaller than at the exposed surface, and the C-RCA shows a lower saturation

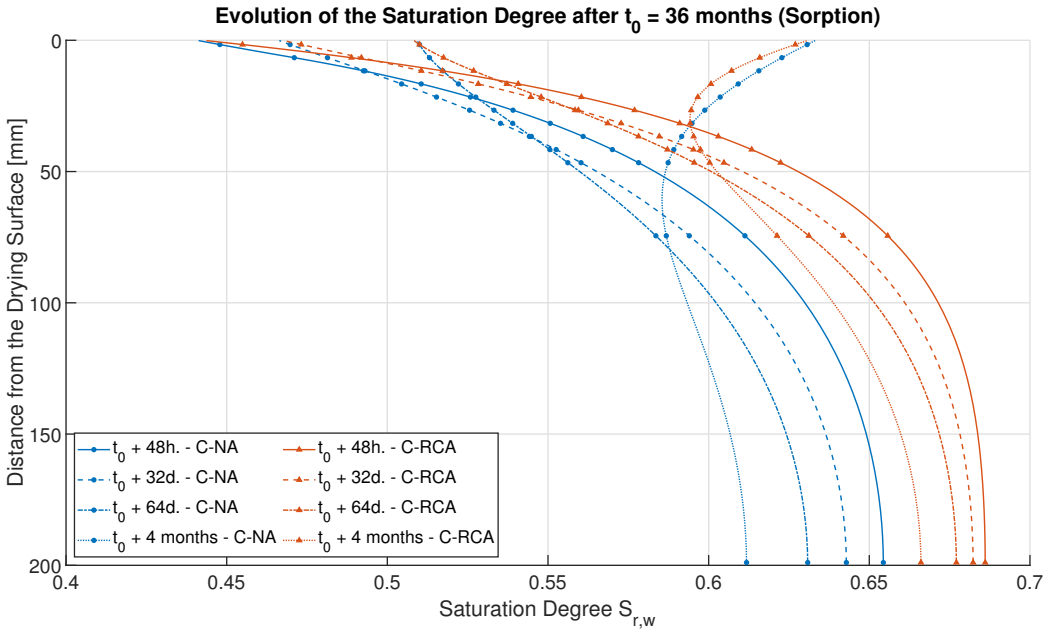

Figure 6: Evolution of the saturation along the height of the sample, starting from t_0=36 months and for a period of four months.

degree than the C-NA in the sorption phase, and a higher saturation degree in the desorption phase. Indeed, its lower relative permeability obviously reduces the exchanges with its environment.

Finally, the middle section of the column was also studied. The amplitudes are once again smaller and the saturation is once again in between the maxima and minima of the last section studied. The same observations as for the previous cross-section studied can be made: the C-RCA's saturation degree varies less than the C-NA's one, and therefore stays higher at all time.

One important aspect to mention is that the closer a section is to the center of the column, the bigger the delay with the exposed surface in terms of sorption/desorption, which was the conclusion obtained from Figure 6.

Figure 8 displays the evolution of the saturation degree, with time and along the discretised width of the column. This graph is helpful to predict the durability of a concrete

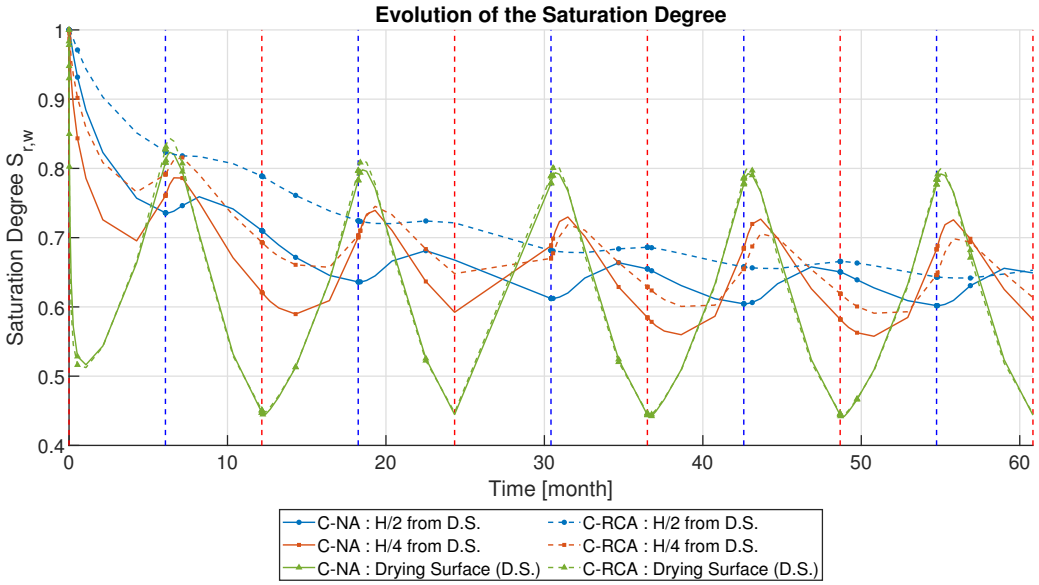

Figure 7: Evolution of the saturation with time, at 3 different depths in the section.

specimen. Indeed, Figure 9 shows that the carbonation rate is maximum around 70% of relative humidity in the environment, under the assumption that the concrete specimen is in equilibrium with its surroundings.

For the interval of temperature studied, that is in between -5°C and 25°C, the suction for a RH of 70% ranges between 44.13MPa and 49.1MPa. Using the water retention curve, it means that the carbonation rate is maximum when the saturation inside the concrete is approximately equal to 65% for the C-NA and 63% for the C-RCA.

At first, the C-RCA and C-NA are submitted to similar saturation variations, even though the saturation degree of the C-RCA decreases more slowly than for the C-NA. This can be confirmed by looking at the saturation of the C-RCA at the middle of the sample (or bottom of the mesh) in Figure 7, which is always above 65%. However, the saturation at the exposed surface of the sample still varies from approximately 45% in desorption to 80% in sorption, and therefore the carbonation rate is still reduced during the sorption as less CO_2 can enter the porous system of the concrete member.

Finally, if we focus on the sections where the saturation degree is approximately 65%, the

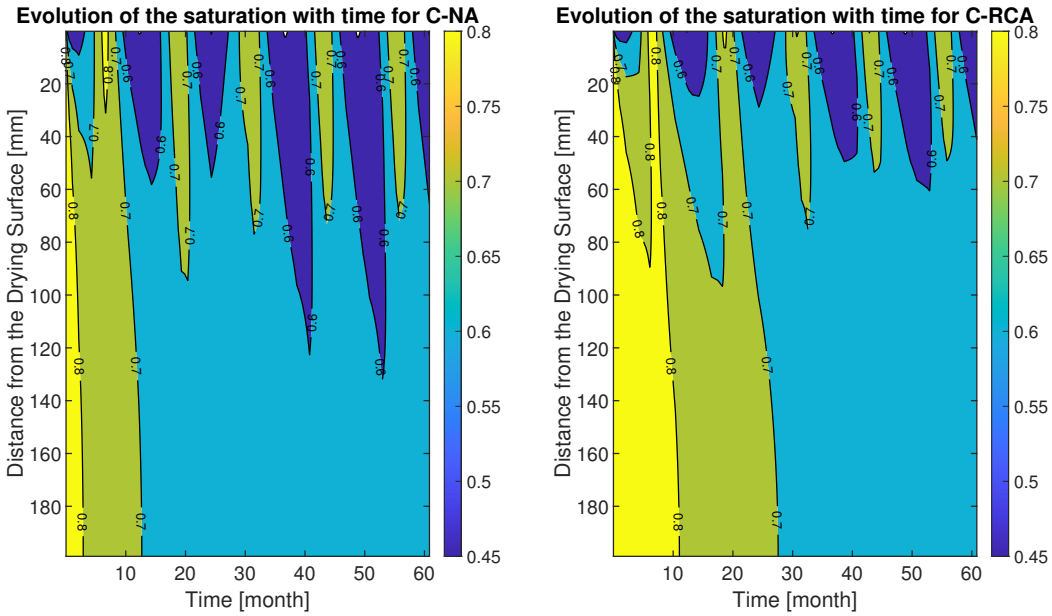

Figure 8: Evolution of the saturation degree with time on the whole section, for variable temperature only.

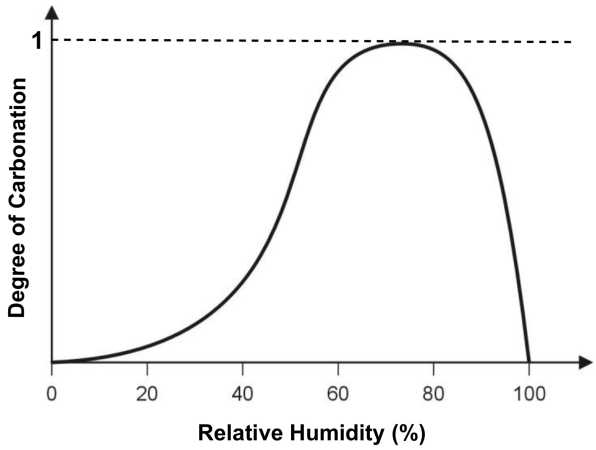

Figure 9: Carbonation rate with respect to the relative humidity of the environment (under equilibrium between the concrete and the environment) (adapted from [48])

C-RCA exhibits a larger zone than for the C-NA, which may be promoting higher carbonation rates according to Figure 9.

Figure 10 represents the same results as Figure 7 as well as three curves that highlight the influence of several transfer properties. Those three curves are based on the C-NA with,

for each one, a property whose value has been changed to the one of the C-RCA: the water retention curve, the porosity or the intrinsic permeability.

One can therefore apprehend which role each transfer property plays in the evolution of the saturation degree. For example, the intrinsic permeability is responsible for the time at which the transfer direction changes (from the inside to the outside and vice versa). It also seems to be one of the causes of a higher saturation degree.

The water retention curve properties also play a major role in the value of the saturation degree, shifting up the curve while keeping it approximately parallel to the original one. This is because the major difference between the two concretes is their air-entry pressure: it causes an initial delay between the two concretes during the first desaturation episode. However, the differences become quite negligible past this period (see Figure 4).

Finally, the porosity is related to the total amount of water content available in the concrete, therefore directly affecting the saturation degree: the bigger the maximum water content, the more time it takes to decrease the saturation degree.

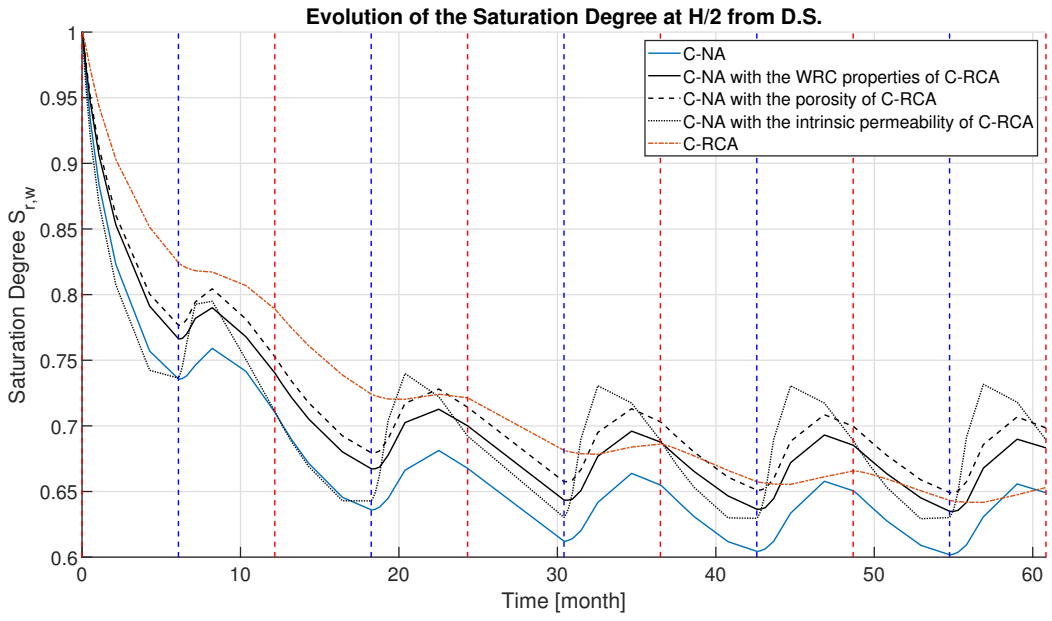

Figure 10: Evolution of the Saturation Degree, at 200mm from the exposed surface, for the two concretes C-NA and C-RCA, and study of the influence of the intrinsic permeability, water retention curve and porosity on the results.

5. Conclusion

Throughout the work achieved in this research, concrete made with recycled concrete aggregates has been characterised in terms of transfer phenomena for the purpose of assessing and trying to predict the durability of this construction material. The scientific question this paper tried to answer is: "Is it possible to efficiently model water transfer in Recycled Aggregate Concrete ?"

Through the multiple experiments conducted, a comparison of two concrete compositions has been done: concrete made with NA (C-NA) and one with RCA (C-RCA). The goal of this research is indeed to highlight the influence of the substitution of NA by RCA. The main results obtained experimentally are:

- Water Absorption by Immersion: the addition of recycled concrete aggregates inside concrete increases its porosity (by 31.5%) and water absorption (by 30.5%). As it was proven in the literature, the Recycled Concrete Aggregates (RCA) alone have a greater water absorption than the Natural Aggregates (NA); therefore, the porosity and water absorption of concrete with RCA increase proportionally to the percentage of RCA used.

- Water permeability: the intrinsic permeability of the C-RCA is 60% smaller than the C-NA. This decreased intrinsic permeability will reduce water movements inside the porous system of concrete, and may be due to the greater water absorption/porosity of the RCA, decreasing the excess water during the mixing stage and therefore possibly increasing the quality of the ITZ.

- Static sorption and desorption: the C-RCA has a smaller air-entry pressure than the C-NA, which means that it will start to desaturate for smaller values of suction than the C-NA. The same logic applies to the sorption. Nonetheless, both water retention curves are relatively close to each other and the properties of the C-RCA with regard to the water retention curves are therefore not as different as one could have imagined.

In addition to the experimental results mentioned above, the numerical modelling part of this research also helped to predict the durability of concrete made from RCA. The numerical application consisted of the study of a column, using experimental properties of the C-NA and C-RCA to model five years of real environmental conditions based on meteorological data available in Belgium. This application showed that the column made from C-RCA has a saturation degree constantly above the one of the C-NA. This may promote a higher carbonation rate or degradation processes where water is required.

The numerical model used proved to be representative of the real transfer conditions between a concrete specimen and its environment, and may be used in many applications. The inputs required can indeed be determined experimentally with classical test procedures. It is therefore an important tool in the assessment of the service life of a concrete member and may help to optimize concrete compositions, or assess the extent of the degradation processes that took place in the member.

As a conclusion, one could state that the use of Recycled Concrete Aggregates (RCA) inside concrete may slightly reduce the durability of concrete due to its composition and physical properties. The application showed that the substitution of the natural aggregates by recycled concrete aggregates leads to a concrete whose saturation is above the saturation of the C-NA, in a range promoting carbonation or other degradation processes.
However, this paper is the first step of a research that studies the chloride ingress inside concrete made from recycled concrete aggregates. The model used is to be developed into a coupled multiscale model for better accuracy.

Nonetheless, further testing and replication of the experiments achieved should be performed. For example, mercury intrusion porosimetry could increase the confidence in the value of the porosity as well as give indications on the pores' distribution. Furthermore,

carbonation experiments and chloride resistance experiments should also be carried out to better differentiate the two compositions in terms of durability.
Numerically, the hysteresis effect between the sorption and desorption observed in the water retention curves could be implemented into the Lagamine software.

Acknowledgements

Funding: This work is supported by the Wallonia regional government (Belgium) in the framework of a FRIA (Fund for Industrial and Agricultural Research) grant.

Competing Interests

The authors declare that they have no known competing financial interests or personal relationships that could have appeared to influence the work reported in this paper.

References

[1] R. A. Patel, P. Janez, J. Diederik, Multi-scale modeling strategies to improve durability models for service life predictions of concrete structures, in: G. D. Schutter, N. D. Belie, A. Janssens, N. V. D. Bossche (Eds.), XIV DBMC - 14th International Conference on Durability of Building Materials and Components, RILEM, Ghent University, Belgium, pp. 309–310.

[2] P. S. Mangat, B. T. Molloy, Prediction of long term chloride concentration in concrete, Materials and Structures 27 (1994) 338–346.

[3] M. Morga, G. C. Marano, Chloride Penetration in Circular Concrete Columns, International Journal of Concrete Structures and Materials 9 (2015) 173–183.

[4] J. Apers, G. de Schutter, Technologie du béton - Chapitre 5 : V Durabilité, volume 5, Groupement Belge du Béton (GBB), Bruxelles, 2018.

[5] Z. P. Bažant, L. J. Najjar, Nonlinear water diffusion in nonsaturated concrete, Materials and Structures 5 (1972) 3–20.

[6] M. Pap, A. Mahler, S. Nehme, Measurement of water retention curve for different concrete mixtures.

[7] M. T. Van Genuchten, A Closed-form Equation for Predicting the Hydraulic Conductivity of Unsaturated Soils, Soil Science Society of America Journal 44 (1980) 892:898.

[8] M. Vinkler, J. L. Vitek, Drying Concrete : Experimental and Numerical Modeling, Journal of Materials in Civil Engineering (2016).

[9] L. J. Parrott, Moisture profiles in drying concrete, Advances in Cement Research 1 (1988) 164–170.

[10] Y. Xi, Z. P. Bažant, H. M. Jennings, Moisture Diffusion in Cementitious Materials - Adsorption Isotherms, Advanced Cement-Based Materials 1 (1994) 248–257.

[11] S. Brunauer, P. H. Emmet, E. Teller, Adsorption of Gases in Multimolecular Layers, Journal of the American Chemical Society 60 (1938) 309–319.

[12] Y. Xi, Z. P. Bažant, L. Molina, H. M. Jennings, Moisture Diffusion in Cementitious Materials - Moisture Capacity and Diffusivity, Advanced Cement-Based Materials 1 (1994) 258–266.

[13] V. Baroghel-Bouny, Water vapour sorption experiments on hardened cementitious materials - Part I : Essential tool for analysis of hygral behaviour and its relation to pore structure, Cement and Concrete Research 37 (2007) 414–437.

[14] P. Gerard, A. Léonard, J.-P. Masekanya, R. Charlier, F. Collin, Study of the soil-atmosphere moisture exchanges through convective drying tests in non-isothermal conditions, International Journal for Numerical and Analytical Methods in Geomechanics 34 (2010) 1297–1320.

[15] J. Hubert, X. F. Liu, F. Collin, Numerical modeling of the long term behavior of Municipal Solid Waste in a bioreactor landfill, Computers and Geotechnics 72 (2016) 152–170.

[16] D. Pedro, J. de Brito, L. Evangelista, Performance of concrete made with aggregates recycled from precasting industry waste: influence of the crushing process, Materials and Structures 48 (2015) 3965–3978.

[17] M. S. de Juan, P. A. Gutiérrez, Study on the influence of attached mortar content on the properties of recycled concrete aggregate, Construction and Building Materials 23 (2009) 872–877.

[18] D. Pedro, J. de Brito, L. Evangelista, Influence of the use of recycled concrete aggregates from different sources on structural concrete, Construction and Building Materials 71 (2014) 141–151.

[19] G. Fathifazl, A. G. Razaqpur, O. B. Isgor, A. Abbas, B. Fournier, S. Foo, Creep and drying shrinkage characteristics of concrete produced with coarse recycled concrete aggregate, Cement and Concrete Composites 33 (2011) 1026–1037.

[20] P. S. Lovato, E. Possan, D. C. C. D. Molin, Â. B. Masuero, J. L. D. Ribeiro, Modeling of mechanical properties and durability of recycled aggregate concretes, Construction and Building Materials 26 (2012) 437–447.

[21] N. Biglarijoo, M. Nili, S. M. Hosseinian, M. Razmara, S. Ahmadi, P. Razmara, Modelling and optimisation of concrete containing recycled concrete aggregate and waste glass, Magazine of Concrete Research 69 (2017) 306–316.

[22] Z. Zhao, L. Courard, F. Michel, S. Delvoie, M. E. Bouarroudj, C. Colman, Properties of concrete with recycled construction and demolition wastes: a research experience in Belgium, Industry-Academia Forum on Advances in Structural Engineering, Tongji University, Shangai (7-9 September 2018), 2018.

[23] S. M. Levy, P. Helene, Durability of recycled aggregates concrete: a safe way to sustainable development, Cement and Concrete Research 34 (2004) 1975–1980.

[24] S. P. Arredondo-Rea, R. Corral-Higuera, J. M. Gómez-Soberón, J. H. Castorena-González, V. Orozco-Carmona, J. L. Almaral-Sánchez, Carbonation Rate and Reinforcing Steel Corrosion of Concretes with Recycled Concrete Aggregates and Supplementary Cementing Materials, International Journal of Electrochemical Science 7 (2012) 1602–1610.

[25] F. Debieb, L. Courard, S. Kenai, R. Degeimbre, Mechanical and durability properties of concrete using contaminated recycled aggregates, Cement and Concrete Composites 32 (2010) 421–426.

[26] D. Chen, S. Mahadevan, Chloride-induced reinforcement corrosion and concrete cracking simulation, Cement and Concrete Composites 30 (2008) 227–238.

[27] F. Collin, X. Li, J. Radu, R. Charlier, Thermo-hydro-mechanical coupling in clay barriers, Engineering Geology 64 (2002) 179–193.

[28] F. Collin, Couplages thermo-hydro-mécaniques dans les sols et les roches tendres partiellement saturés, Ph.D. thesis, Uliège University, 2003.

[29] T. C. Hansen, Recycled aggregates and recycled aggregate concrete second state-of-the-art report developments 1945-1985, Materials and Structures 19 (1986) 201–246.

[30] S. Nagataki, A. Gokce, T. Saeki, M. Hisada, Assessment of recycling process induced damage sensitivity of recycled concrete aggregates, Cement and Concrete Research 34 (2004) 965–971.

[31] A. Rao, K. N. Jha, S. Misra, Use of aggregates from recycled construction and demolition waste in concrete, Resources, Conservation and Recycling 50 (2007) 71–87.

[32] J. Xiao, J. Ying, L. Shen, FEM simulation of chloride diffusion in modeled recycled aggregate concrete, Construction and Building Materials 29 (2012) 12–23.

[33] A. Akbarnezhad, K. C. G. Ong., C. T. Tam, M. H. Zhang, Effects of the Parent Concrete Properties and Crushing Procedure on the Properties of Coarse Recycled Concrete Aggregates, Journal of Materials in Civil Engineering 25 (2013) 1795–1802.

[34] H. Hussain, D. Levacher, J.-L. Quenec'h, A. Bennabi, F. Bouvet, Valorisation des aggrégats issus de bétons de démolition dans la fabrication de nouveaux bétons, Sciences et techniques 19 (2000) 17–22.

[35] J. García-González, D. Rodríguez-Robles, A. Juan-Valdés, J. M. M. del Pozo, M. I. Guerra-Romero, Pre-Saturation Technique of the Recycled Aggregates: Solution to the Water Absorption Drawback in the Recycled Concrete Manufacture, Materials 7 (2014) 6224–6236.

[36] P. Belin, G. Habert, M. Thiery, N. Roussel, Cement paste content and water absorption of recycled concrete coarse aggregates, Materials and Structures 47 (2014) 1451–1465.

[37] M. V. A. Florea, H. J. H. Brouwers, Properties of various size fractions of crushed concrete related to process conditions and re-use, Cement and Concrete Research 52 (2013) 11–21.

[38] H. Guo, C. Shi, X. Guan, J. Zhu, Y. Ding, T.-C. Ling, H. Zhang, Y. Wang, Durability of Recycled Aggregate Concrete - A Review, Cement and Concrete Composites 89 (2018) 251–259.

[39] J. M. Gómez-Soberón, Porosity of recycled concrete with substitution of recycled concrete aggregate - An experimental study, Cement and Concrete Research 32 (2002) 1301–1311.

[40] K. Deodonne, Études des caractéristiques physico-chimiques de bétons de granulats recyclés et de leur impact environnemental, Ph.D. thesis, Université de Strasbourg, 2015.

[41] C. Hamza, S. Bouchra, B. Mostapha, B. Mohamed, Formulation of Ordinary Concrete using the Dreux-Gorisse Method, Procedia Structural Integrity 28 (2020) 430–439.

[42] S. J. Kowalski, Thermomechanics of Drying Processes, Springer-Verlag Berlin Heidelberg GmbH, 2003.

[43] A. Dassargues, Hydrogéologie Appliquée : Science et ingénierie des eaux souterraines, Dunod, 2020.

[44] J. Hubert, Experimental and numerical study of cracking during the drying of porous materials : application to the fields of chemical engineering and geomechanics, Ph.D. thesis, ULiège University, 2018.

[45] P. K. Mehta, P. J. M. Monteiro, Effect of aggregate, cement, and mineral admixtures on the microstructure of the transition zone, Materials Research Society Symp. Proc. 114 (1988) 65–75.

[46] A. Bentur, I. Odler, Development and nature of interfacial microstructure, in: J. Maso (Ed.), Interfacial Transition Zone in Concrete, RILEM REPORT, volume 11, E & FN Spon, 1996, pp. 21–50.

[47] WeatherOnline, Bruxelles Aéroport - Humidité Relative, 2020. https://www.wofrance.fr/weather/maps/city?LANG=fr&WMO=06451&ART=RLF&CONT=euro&R=0&LEVEL=150&REGION=0003&LAND=BX&NOREGION=1&MOD=&TMX=&TMN=&SON=&PRE=&MONAT=&OFFS=&SORT=. Accessed: 1 May 2020.

[48] L. Bertolini, B. Elsener, P. Pedeferri, R. P. Polder, Corrosion of Steel in Concrete, WILEY-VCH Verlag GmbH and Co. KGaA, Weinheim, 2004.